

Multi-timescale representation learning in LSTM Language Models

Shivangi Mahto¹, Vy A. Vo², Javier S. Turek², and Alexander G. Huth^{1,3}

¹Department of Computer Science, The University of Texas at Austin

²Brain-Inspired Computing Lab, Intel Labs

³Department of Neuroscience, The University of Texas at Austin

shivangi@utexas.edu, {vy.vo, javier.turek}@intel.com, huth@cs.utexas.edu

Abstract

Although neural language models are effective at capturing statistics of natural language, their representations are challenging to interpret. In particular, it is unclear how these models retain information over multiple timescales. In this work, we construct explicitly multi-timescale language models by manipulating the input and forget gate biases in a long short-term memory (LSTM) network. The distribution of timescales is selected to approximate power law statistics of natural language through a combination of exponentially decaying memory cells. We then empirically analyze the timescale of information routed through each part of the model using word ablation experiments and forget gate visualizations. These experiments show that the multi-timescale model successfully learns representations at the desired timescales, and that the distribution includes longer timescales than a standard LSTM. Further, information about high-, mid-, and low-frequency words is routed preferentially through units with the appropriate timescales. Thus we show how to construct language models with interpretable representations of different information timescales.

1 Introduction

Effective language models should capture the statistical properties of natural language, including information that varies at multiple timescales. For example, syntactic effects evolve at the timescale of words, whereas semantics, emotions, and narratives can evolve at much longer timescales of tens to hundreds or thousands of words. The importance of long timescale information is evident in results showing that neural networks have outperformed classical n -gram models on many language modeling benchmarks (Melis et al., 2019; Krause et al., 2019; Dai et al., 2019). This difference is attributed to these networks' ability to capture long timescale

dependencies that are impossible for n -gram models. Yet it is difficult to interpret how neural language models represent information at different timescales, and unclear how these timescale representations should be controlled to yield better or more interpretable models.

One popular architecture for neural language models is recurrent neural networks, in particular Long Short-Term Memory (LSTM) (Hochreiter and Schmidhuber, 1997; Merity et al., 2018; Melis et al., 2018). Efforts to interpret the representations learned by LSTMs using probing tasks have shown that LSTM language models are capable of learning both short timescale information about word order (i.e., syntactic information) (Adi et al., 2017; Linzen et al., 2016), and long timescale semantic information (Zhu et al., 2018; Conneau et al., 2018; Gulordava et al., 2018). Other methods have attempted to interpret the timescale of LSTM representations using predictive models of brain responses to natural language (Jain and Huth, 2018; Toneva and Wehbe, 2019). Yet the question of how and where information about different timescales is maintained in LSTM representations still does not have a satisfying answer.

One alternative to interpreting representations in existing models is to construct language models in which different layers or groups of units are explicitly constrained to operate at different timescales. Several approaches have been proposed for building such explicitly multi-timescale models, including updating different groups of units at different intervals (El Hihi and Bengio, 1996; Koutnik et al., 2014; Liu et al., 2015; Chung et al., 2017), gating units across layers (Chung et al., 2015), and including explicit control of the input and forget gates that determine how information is stored and removed from memory (Xu et al., 2016; Shen et al., 2018; Tallec and Ollivier, 2018). These approaches ease interpretation by controlling the timescales

represented by different units. Yet this raises a new concern: unlike standard LSTMs, explicitly multi-timescale models are unable to flexibly learn the statistics of natural language. This can decrease the performance of these models (Kádár et al., 2018) and diminish their utility. Thus, when constructing explicitly multi-timescale language models it is important to consider which timescales are present in natural language.

Lin and Tegmark (2016) quantified the distribution of timescales in natural language by measuring the mutual information between tokens as a function of the distance between them. They observed that mutual information decays as a power law, which is common to many hierarchical structures (Lin and Tegmark, 2016; Sainburg et al., 2019). It would be desirable for a language model to retain temporal information that mimics these statistics. However, it is not clear how to attain power law using LSTMs, which are fundamentally designed to decay information exponentially across time (Tallec and Ollivier, 2018).

In this work, we present a method to control the timescales of information represented by each unit of an LSTM language model, resulting in interpretable multi-timescale representations. Building on the theoretical grounding of Tallec and Ollivier (2018), we quantify the timescale represented in each unit using forget gate activations. We use this framework to analyze an existing LSTM language model (Merity et al., 2018) and show how different layers of the model retain information across time. Next, we use this framework to construct explicitly multi-timescale language models where the timescale of each LSTM unit is controlled by setting the forget and input gate biases. To determine the distribution of timescales within this model we used a prior that mimics the power law statistical properties of natural language (Lin and Tegmark, 2016) through a combination of exponential timescales. Finally, we show that this prior creates interpretable representations in which long and short timescale information is selectively routed into different parts of the network.

2 Multi-timescale Language Models

2.1 Timescale of information

We are interested in understanding and quantifying the timescale of information in LSTM-based language models. The timescale is directly related to the memory mechanism employed by the LSTM,

which involves the LSTM cell state c_t , input gate i_t and forget gate f_t ,

$$\begin{aligned} i_t &= \sigma(W_{ix}x_t + W_{ih}h_t + b_i) \\ f_t &= \sigma(W_{fx}x_t + W_{fh}h_t + b_f) \\ \tilde{c}_t &= \tanh(W_{cx}x_t + W_{ch}h_t + b_c) \\ c_t &= f_t \odot c_{t-1} + i_t \odot \tilde{c}_t, \end{aligned}$$

where x_t is the input at time t , h_t is the hidden state, $W_{ih}, W_{ix}, W_{fh}, W_{fx}, W_{ch}, W_{cx}$ are the different weight matrices and b_i, b_f, b_c the respective biases. $\sigma(\cdot)$ and $\tanh(\cdot)$ represent element-wise sigmoid and hyperbolic tangent functions. Input and forget gates control the flow of information in and out of memory. The forget gate f_t controls how much memory from the last time step c_{t-1} is carried forward to the current state c_t . The input gate i_t controls how much information from the input x_t and hidden state h_t at the current timestep is stored in memory for subsequent timesteps.

To examine representational timescales, consider a “free input” regime in which there is only null input to the LSTM after timestep t_0 , i.e., $x_t = 0$ for $t > t_0$. Ignoring information leakage through the hidden state, i.e., assuming $W_{ch} = 0$, $b_c = 0$, and $W_{fh} = 0$, the cell state update becomes

$$c_t = f_t \odot c_{t-1}.$$

For $t > t_0$, it can be further simplified as

$$\begin{aligned} c_t &= f_0^{t-t_0} \odot c_0 \\ &= c_0 \odot e^{(\log f_0)(t-t_0)}, \end{aligned} \quad (1)$$

where $c_0 = c_{t_0}$ is the cell state at t_0 , and $f_0 = \sigma(b_f)$ is the value of the forget gate, which depends only on the forget gate bias b_f here. Equation (1) shows that LSTM memory exhibits exponential decay with characteristic *forgetting time*,

$$T = \frac{-1}{\log f_0} = \frac{1}{\log(1 + e^{-b_f})}. \quad (2)$$

That is, values in the cell state tend to shrink by a factor of e every T timesteps. We refer to the forgetting time in Equation (2) as the timescale of information represented by an LSTM unit.

2.2 Estimating the timescale of information

Our definition for the timescale of a LSTM unit in Equation (2) above applies in the free regime which is dominated by the forget gate bias b_f . Beyond this simple case, we can estimate the timescale for

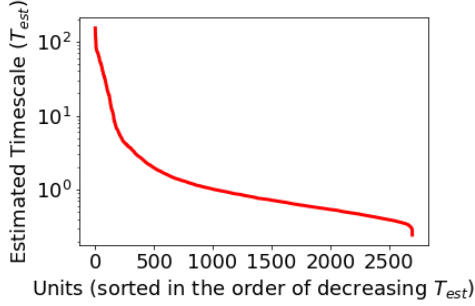


Figure 1: Estimated timescales across units in the model from Merity et al. (2018). The majority of units have estimated timescales that are less than 20. The model learned to process information for timescales as long as 150 timesteps.

a LSTM unit by measuring the average forget gate values over a set of real test sequences,

$$T_{est} = \frac{-1}{\log \bar{f}}, \quad (3)$$

where $\bar{f} = \frac{1}{KN} \sum_{j=1}^N \sum_{t=1}^K f_t^j$ where f_t^j is the forget gate value of the unit at t th timestep for j th test sentence. N is the total number of test sentences and K is the length of test sentences.

Figure 1 shows estimated timescales in the LSTM language model from Merity et al. (2018) trained on Penn Treebank (Marcus et al., 1999; Mikolov et al., 2011). These timescales lie between 0 and 150 timesteps, with more than 90% of timescales being less than 10 timesteps, indicating that this network skews its forget gates to process shorter timescales during training. This resembles the findings by Khandelwal et al. (2018), which showed that the model’s sensitivity is reduced for information farther than 20 timesteps in the past. Ideally, we would like to control the timescale of each unit to counter this training effect and select globally a distribution that follows from natural language data.

2.3 Controlling the timescale of information

Following the analysis in Section 2.1, the desired timescale $T_{desired}$ for an LSTM unit can be controlled by setting the forget gate bias to the value

$$b_f = -\log\left(e^{\frac{1}{T_{desired}}} - 1\right). \quad (4)$$

The balance between forgetting information from the previous timestep and adding new information from the current timestep is controlled by the relationship between forget and input gates. To maintain this balance we set the input gate bias b_i to the

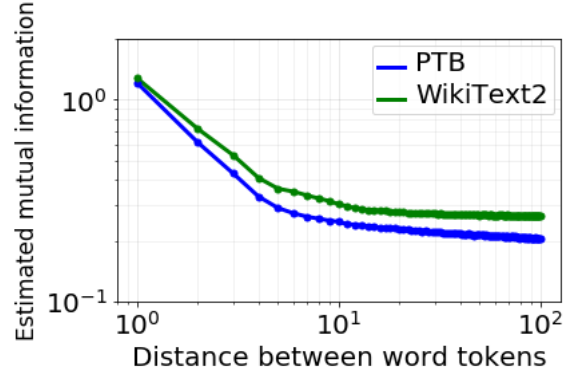


Figure 2: Estimated mutual information of tokens in Penn Treebank (PTB) and WikiText-2 datasets.

opposite value of the forget gate, i.e., $b_i = -b_f$. This ensures that the relation $i_t \approx 1 - f_t$ holds true. Importantly, these bias values remain fixed (i.e. are *not* learned) during training, in order to keep the desired timescale distribution across the network.

2.4 Assigning a distribution of timescales for language modeling

Ideally, we would like to select the distribution of timescales across LSTM units to match the statistics of natural language. It is well known that natural language contains a mixture of different types of dependence that evolve at different timescales (Lang et al., 1990; Daubechies, 1990; El Hahi and Bengio, 1996). All of these effects can be summarized by examining the mutual information between tokens as a function of their separation, which has been observed to approximately follow a power law decay (Lin and Tegmark, 2016). In Figure 2 we reproduce this result, showing the power law decay of mutual information for the Penn Treebank and WikiText-2 (Merity et al., 2017) datasets. This suggests that the distribution of timescales should approximate power law decay across time.

From Equation (1) we see that LSTM memory tends to decay exponentially. Thus, we will approximate the power law decay seen in natural language using a mixture of exponential functions. Let us assume that the timescale T for each unit is drawn from a distribution $P(T)$. We want to define $P(T)$ such that the expected value over T of the function $e^{-t/T}$ approximates a power law decay t^{-d} for some constant d ,

$$t^{-d} \propto \mathbb{E}_T[e^{-t/T}] = \int_0^\infty P(T)e^{-t/T} dT. \quad (5)$$

Noting the similarity between this equation and

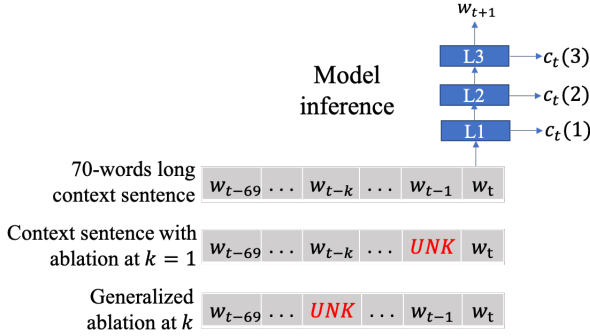


Figure 3: Word ablation experiment. For each input context sentence and each value of k from $k = 1$ to $k = t - 1$, the word k timesteps before the current timestep t is replaced with *UNK*. The cell state vectors at t are then extracted. The impact of each word ablation is measured as the distance between the original cell state vector and the cell state vector after ablation (Eq. 6).

the Laplace transform, we can solve this problem to find that $P(T)$ is an *Inverse Gamma distribution* with shape parameter $\alpha = d$ and scale parameter $\beta = 1$. The probability density function of the inverse gamma distribution is given as $P(T; \alpha, \beta) = \frac{\beta^\alpha}{\Gamma(\alpha)} (1/T)^{\alpha+1} \exp(-\beta/T)$. Selecting exponential timescales according to this distribution should thus enable us to approximate the power law temporal dependencies of natural language using an LSTM.

2.5 Visualizations to interpret the timescale of each LSTM unit

Controlling the timescale of each unit in an LSTM language model enables us to obtain interpretable representations. To understand the effects of our manipulations, we use several techniques to interpret and visualize the timescale of information passing through each unit.

Forget gate visualization. For each LSTM unit, we compute the mean forget gate value across different timesteps for a test sentence. We then sort the units according to their mean forget gate values. High mean forget gate values imply that a unit retains information from the past over longer timescales, while low mean forget gate values imply that a unit only maintains shorter timescale information. This visualisation serves to check whether the assigned timescale relates with the forget gate values of the unit or not.

Word ablation during inference. The decay of information in the cell state of an LSTM layer is

another indicator of the timescale of information passing through that layer. We visualize the rate of information decay by ablating words (i.e. replace them with *UNK*) during inference, and then measuring the effect on subsequent cell states. This procedure is depicted in Figure 3.

The impact of ablating word w_{t-k} on the cell state of layer i is called $\Delta c_k(i)$. Specifically, $\Delta c_k(i)$ is the normalized L2 norm over the difference of cell states in layer i with and without ablating the word k timesteps away from the current timestep t in the sentence, or

$$\Delta c_k(i) = \frac{1}{L} \sum_{t=1}^L \frac{\|c_t^k(i) - c_t(i)\|_2}{\|c_t(i)\|_2}, \quad (6)$$

where $c_t^k(i)$ is the cell state vector of layer i at word t with word $t - k$ ablated, $c_t(i)$ is the cell state vector of layer i without ablation, and L is the length of the input test sentence. In our experiments, we estimate $\Delta c_k(i)$ for k ranging from 0 to maximum length of the input sentence and average it over all the test sentences.

3 Evaluation

3.1 Experimental Setup

We experimentally evaluated the effectiveness of our explicit multi-timescale language model on the Penn Treebank (PTB) (Marcus et al., 1999; Mikolov et al., 2011) and WikiText-2 (WT2) (Merity et al., 2017) datasets. PTB contains a vocabulary of 10K unique words, with 930K tokens in the training, 200K in validation, and 82K in test data. WT2 is a larger dataset with a vocabulary size of 33K unique words, with almost 2M tokens in the training set, 220K in the validation set, and 240K in the test set.

We compared two language models: a standard stateful LSTM language model (Merity et al., 2018) as the baseline, and our multi-timescale language model. Both models comprise three LSTM layers with 1150 units in the first two layers and 400 units in the third layer, with an embedding size of 400. The input and output embeddings were tied. All models were trained using SGD followed by non-monotonically triggered ASGD for 1000 epochs. Training sequences were of length 70 with a probability of 0.95 and 35 with a probability of 0.05. During inference, all test sentences were of length 70. For training, all embedding weights were uniformly initialized in the interval $[-0.1, 0.1]$. All

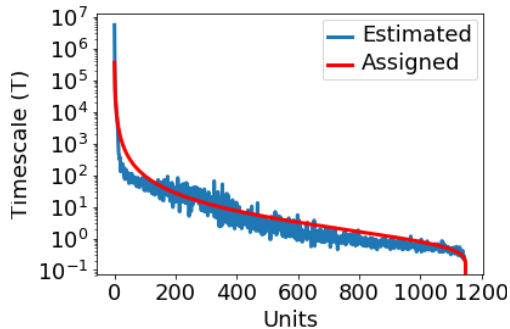


Figure 4: Estimated timescale is highly correlated with assigned timescale, shown for all 1150 units in LSTM layer 2 of the multi-timescale language model.

weights and biases of the LSTM layers were uniformly initialized between $[-\frac{1}{H}, \frac{1}{H}]$ where H is the output size of the respective layer.

Multi-timescale language models have the same architecture and training schedule as the baseline model, except for the forget and input gate bias values for the first two LSTM layers. In order to get representations for short timescale information, we assigned timescale $T = 3$ to half of the units and timescale $T = 4$ to the rest for layer 1. Using Equation (4), the corresponding forget and input gate bias values for units with timescale $T = 3$ were fixed to 0.92 and -0.92 , whereas for the units with timescale $T = 4$, they were fixed to 1.25 and -1.25 . For layer 2, we assigned timescales to each unit by selecting values from an Inverse Gamma distribution. These timescales were then used to compute the forget and input biases for each unit. We selected the best shape parameter α for the inverse gamma distribution (which is equal to the exponent d in the corresponding power law) by testing several different values, and found that $\alpha = 0.56$ works best for our models. This parameter sets 80% units of layer 2 to have timescales less than 20 and the rest to have higher timescales ranging up to the thousands. Biases in the third LSTM layer were not fixed, as we found that changes here had little effect on the network. Further details about the selection of these parameters is available in the supplementary material.

3.2 Experimental Results

3.2.1 Relationship between forget gate and timescale

In Section 2.3, we showed that the forget gate bias controls the timescale of the unit, and derived a distribution of assigned timescales for the multi-timescale language model. After training this

model, we tested whether this control was successful by estimating the empirical timescale of each unit based on their mean forget gate values using Equation (2). Figure 4 shows that the assigned and estimated timescales in layer 2 are strongly correlated. This demonstrates that the timescale of an LSTM unit can be effectively controlled by the forget gate bias.

3.2.2 Forget gate visualisation

To further examine representational timescales, we next visualized forget gate values of units from all three layers of both the multi-timescale and baseline language models as described in Section 2.5. The goal is to compare the distribution of these forget gate values across the two language models, and to assess how these values change over time for a given input.

First, we sorted the LSTM units of each layer according to their mean forget gate values over a test sequence. For visualization purposes, we then downsampled these values by calculating the average forget gate value of every 10 consecutive sorted units for each timestep. Heat maps of these sorted and down-sampled forget gate values are shown in Figure 5. The horizontal axis shows timesteps (words) across a sample test sequence, and the vertical axis shows different units. Units with average forget gate values close to 1.0 (bottom) are retaining information across many timesteps, i.e. they are capturing long timescale information. Figure 5 shows that the baseline language model contains fewer long timescale units than the multi-timescale language model. They are also more evenly distributed across the layers than the multi-timescale language model. Figure 5b also shows the (approximate) assigned timescales for units in the multi-timescale language model. As expected, layer 1 contains short timescales and layer 2 contains a range of both short and long timescales. Layer 1 units with short (assigned) timescales have smaller forget gate values across different timesteps. In layer 2, we observe that units with large assigned timescale have higher mean forget gate values across different timesteps, for example the units with assigned timescale of 362 in 5b have forget gate values of almost 1.0 across all timesteps. Similar to the previous analysis, this demonstrates that our method is effective at controlling the timescale of each unit, and assigns a different distribution of timescales than the baseline model.

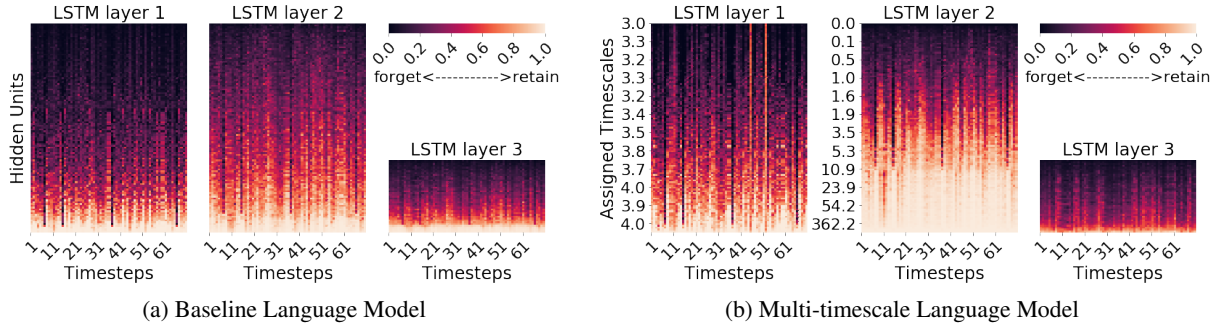


Figure 5: Forget gate values of LSTM units for a test sentence from the PTB dataset. Units are sorted top to bottom by increasing mean forget gate value, and averaged in groups of 10 units to enable visualization. Figure 5b also shows average assigned timescale (rounded off) of the units.

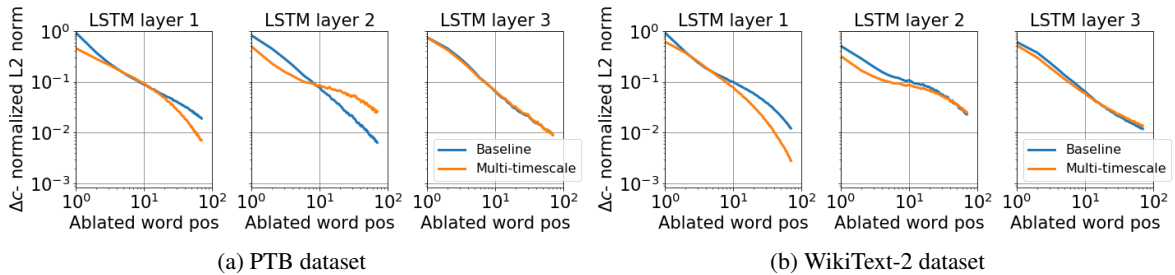


Figure 6: Change in cell state of all the three layers for both the baseline and Multi-timescale language models in word ablation experiment. A curve with a steep slope indicates that cell state difference decays quickly over time, suggesting that the LSTM layer retains information of shorter timescales.

3.2.3 Word ablation

Another way to interpret timescale of information retained by the layers is to visualize the decay of information in the cell state over time. We estimated this decay with word ablation experiments as described in Section 2.5.

In Figure 6, we show the normalized cell state difference averaged across test sentences for all three layers of both baseline (blue) and multi-timescale (orange) models. In the PTB dataset, information in layer 1 of the baseline model decays more slowly than in layer 2. In this case, layer 2 of the baseline model retains shorter timescale information than layer 1. In the WikiText-2 dataset, the difference between layer 1 and layer 2 of the baseline model is inverted, with layer 2 retaining longer timescale information. However, in the multi-timescale model the trend is nearly identical for both datasets, with information in layer 2 decaying more slowly than layer 1. This is expected for our multi-timescale model, which we designed to have short timescale dependencies in layer 1 and longer timescale dependencies in layer 2. Furthermore, the decay curves are very simi-

lar across datasets for the multi-timescale model, but not for the baseline model, demonstrating that controlling the timescales gives rise to predictable behavior across layers and datasets. Layer 3 has similar cell state decay rate across both models. In both models, layer 3 is initialized randomly, and we expect its behavior to be largely driven by the language modeling task.

Next, we explored the rate of cell state decay across different groups of units in layer 2 of the multi-timescale language model. We first sorted the layer 2 units according to their assigned timescale and then partitioned these units into groups of 100 before estimating the cell state decay curve for each group. As can be seen in Figure 7, units with a shorter average timescale have faster decay rates, whereas units with longer average timescale have slower information decay. While the previous section demonstrated that our manipulation could control the forget gate values, this result demonstrates that we can directly influence how information is retained in the LSTM cell states.

Dataset	Model	above 10K	1K-10K	100-1K	below 100	All tokens
PTB	Baseline	6.82	27.77	184.19	2252.50	61.40
	Multi-timescale	6.84	27.14	176.11	2100.89	59.69
	Mean diff.	-0.02	0.63	8.08	152.03	1.71
	95% CI	[-0.06, 0.02]	[0.38, 0.88]	[6.04, 10.2]	[119.1, 186.0]	[1.41, 2.02]
WT2	Baseline	7.49	49.70	320.59	4631.08	69.88
	Multi-timescale	7.46	48.52	308.43	4318.72	68.08
	Mean diff.	0.03	1.17	12.20	312.13	1.81
	95% CI	[0.01, 0.06]	[0.83, 1.49]	[9.96, 14.4]	[267.9, 356.3]	[1.61, 2.01]

Table 1: Perplexity of the multi-timescale and baseline models for tokens across different frequency bins for the Penn TreeBank (PTB) and WikiText-2 (WT2) test datasets. We also report the mean difference in perplexity (baseline - multi-timescale) across 10,000 bootstrapped samples, along with the 95% confidence interval (CI).

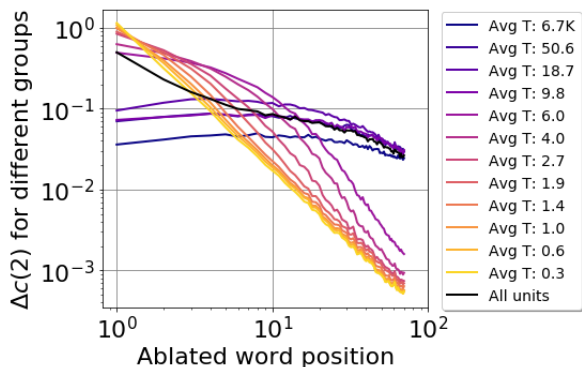


Figure 7: Change in cell states of 100-unit groups having different average timescale of layer 2 in Multi-timescale model in word ablation experiment for PTB dataset. As the assigned timescale to the group decreases the slope of the curve decreases indicating retained information of smaller timescale.

3.2.4 Language modeling performance

One potential downside of constructing explicitly multi-timescale language models is that they may perform worse than ordinary language models, rendering their utility questionable. We attempted to address this issue by using a prior on the distribution across timescales that matches the statistical temporal dependencies of natural language. To test whether this effort was successful at building an effective model, we compared language modeling performance between the baseline and multi-timescale models by computing perplexity on the test portion of each dataset. Results are shown in Table 1. Here we see that the multi-timescale language model significantly outperforms the baseline model for both datasets by an average margin of 1.75 perplexity, demonstrating that the explicitly multi-timescale language model is actually better.

From the earlier forget gate visualizations and

word ablation tests, we saw that the multi-timescale model seemed to contain larger representations of very long timescale than did the baseline model. Thus the small performance advantage of the multi-timescale model might be due to it better capturing long timescale information. To test this, we investigated how language model performance differed for predicting words that appear with different frequencies. It has been shown that common words rely mostly on short timescale information, whereas rare words require longer timescale information (Khandelwal et al., 2018). Thus if the multi-timescale model contains more long timescale information, it should give larger improvements to model performance for infrequent words.

We divided the words in the test dataset into 4 bins depending on their frequencies in the training data: a) greater than 10,000 occurrences; b) between 1000 and 10,000; c) between 100 and 1000; and d) extremely rare words with less than 100 occurrences. Then we compared performance of the models for test words belonging to each frequency bin in Table 1. The multi-timescale model performed significantly better than baseline in both datasets for the 3 less frequent bins, with increasing difference for the less frequent words. This result suggests that the performance advantage of the multi-timescale model is highest for words that require very long timescale information.

We assessed statistical significance of the differences in performance between models using a bootstrap procedure. Test data were divided into 100-word sequences and resampled with replacement 10,000 times. For each sample, we computed the difference in model perplexity (baseline - multi-timescale) for each word frequency bin and across all words. We report the 95% confidence inter-

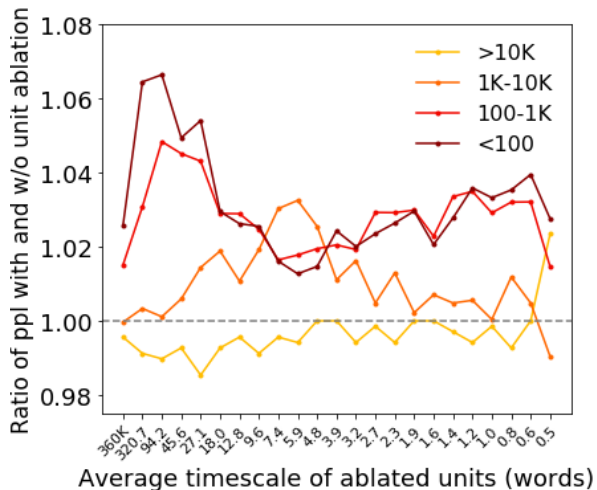


Figure 8: Information routing across different units of the multi-timescale LSTM for PTB dataset. Each line shows results for words in a different frequency bin. The ordinate axis shows the ratio of model perplexity with and without ablation of a group of 50 LSTM units, sorted and grouped by assigned timescale. Ratios above 1 indicate a decrease in performance following ablation, suggesting that the ablated units are important for predicting words in the given frequency bin. Abscissa shows the average timescale of each group.

vals (CIs) of the perplexity difference in Table 1. The difference between models is significant at a level of $p < 0.05$ if the CI does not overlap with 0. The multi-timescale model thus has a significantly lower perplexity across all frequency bins, except for the highest frequency words in PTB. In separate tests we showed that these results are also robust to random initialization when training the model 5.3.

3.2.5 Routing of information through LSTM units with different timescales

Our previous results showed that we were able to successfully control the timescales of different units in our multi-timescale model, and that this did not cause model performance to suffer (in fact, performance improved). However, we have not yet shown that the representations that this model learns for different timescales are interpretable. For these representations to be interpretable, we would expect that different types of information are routed through the units that were assigned different timescales. To test this, we divided the test data into word frequency bins for which different timescales of information should be important. For example, if long timescale information is particularly important for low frequency words, then we would expect that information about those words

is selectively routed through the units that were assigned long timescales. We tested the importance of LSTM units with different assigned timescales for words in each frequency bin by selectively ablating those units during inference, and then measuring the effect on prediction performance.

We divided the LSTM units from layer 2 of the multi-timescale model into 23 groups of 50 consecutive units, sorted by assigned timescale. We ablated one group of units at a time by explicitly setting their output to 0, while keeping the rest of the units active. We then computed the model perplexity for different word frequency bins, and plotted the ratio of the perplexity with and without ablation. If performance gets worse for a particular frequency bin when ablating a particular group of units, it implies that the ablated units are routing information corresponding to that timescale.

Figure 8 shows this ratio across all frequency bins and groups for the PTB dataset (similar results for WikiText-2 are shown in the supplement). Ablating units with a long timescales (20-300 words) causes performance to degrade the most for low frequency words (below 100 and 1K-10K); ablating units with medium timescales (5-10 words) worsens performance for medium frequency words (1k-10k); and ablating units with the shortest timescales (<1 word) resulted in worse performance on the highest frequency words. These results demonstrate that timescale-dependent information is routed through different units in this model, suggesting that the representations that are learned for different timescales are interpretable.

4 Conclusion

In this paper, we presented a mechanism to interpret and control the timescale of information routing through an LSTM unit via the input and forget gate biases. We first examined the timescale of information flowing through a standard LSTM language model and found that most units preferred short timescale information. We designed a multi-timescale language model where timescales in the middle layer were assigned based on an inverse gamma distribution, a prior that we introduce based on nature language statistics. We used several methods including forget gate visualization, unit ablation, and word ablation to study and compare timescales of information in our model and a standard LSTM. The results showed that our model was successful in learning the representations of vari-

ous timescales, including longer timescales than the standard model. These results demonstrate that our explicit multi-timescale LSTM language model can be a useful tool for studying representations of different timescales in natural language.

References

- Yossi Adi, Einat Kermany, Yonatan Belinkov, Ofer Lavi, and Yoav Goldberg. 2017. [Fine-grained analysis of sentence embeddings using auxiliary prediction tasks](#). In *International Conference on Learning Representations*.
- Junyoung Chung, Sungjin Ahn, and Yoshua Bengio. 2017. [Hierarchical multiscale recurrent neural networks](#). In *Proceedings of the 5th International Conference on Learning Representations*.
- Junyoung Chung, Aglar Glehre, Kyunghyun Cho, and Yoshua Bengio. 2015. [Gated feedback recurrent neural networks](#). In *ICML*, pages 2067–2075.
- Alexis Conneau, Germán Kruszewski, Guillaume Lample, Loïc Barrault, and Marco Baroni. 2018. [What you can cram into a single vector: Probing sentence embeddings for linguistic properties](#). In *Proceedings of the 56th Annual Meeting of the Association for Computational Linguistics (Volume 1: Long Papers)*, pages 2126–2136.
- Zihang Dai, Zhilin Yang, Yiming Yang, Jaime G Carbonell, Quoc Le, and Ruslan Salakhutdinov. 2019. [Transformer-xl: Attentive language models beyond a fixed-length context](#). In *Proceedings of the 57th Annual Meeting of the Association for Computational Linguistics*, pages 2978–2988.
- Ingrid Daubechies. 1990. [The wavelet transform, time-frequency localization and signal analysis](#). *IEEE transactions on information theory*, 36(5):961–1005.
- Salah El Hahi and Yoshua Bengio. 1996. [Hierarchical recurrent neural networks for long-term dependencies](#). In *Advances in neural information processing systems*, pages 493–499.
- Kristina Gulordava, Piotr Bojanowski, Édouard Grave, Tal Linzen, and Marco Baroni. 2018. [Colorless green recurrent networks dream hierarchically](#). In *Proceedings of the 2018 Conference of the North American Chapter of the Association for Computational Linguistics: Human Language Technologies, Volume 1 (Long Papers)*, pages 1195–1205.
- Sepp Hochreiter and Jürgen Schmidhuber. 1997. [Long short-term memory](#). *Neural Computation*, 9(8):1735–1780.
- Shailee Jain and Alexander Huth. 2018. [Incorporating context into language encoding models for fmri](#). In *Advances in neural information processing systems*, pages 6628–6637.
- Ákos Kádár, Marc-Alexandre Côté, Grzegorz Chrupała, and Afra Alishahi. 2018. [Revisiting the hierarchical multiscale LSTM](#). In *Proceedings of the 27th International Conference on Computational Linguistics*, pages 3215–3227, Santa Fe, New Mexico, USA. Association for Computational Linguistics.
- Urvashi Khandelwal, He He, Peng Qi, and Dan Jurafsky. 2018. [Sharp nearby, fuzzy far away: How neural language models use context](#). In *Proceedings of the 56th Annual Meeting of the Association for Computational Linguistics (Volume 1: Long Papers)*, pages 284–294, Melbourne, Australia. Association for Computational Linguistics.
- Jan Koutník, Klaus Greff, Faustino Gomez, and Jürgen Schmidhuber. 2014. [A clockwork rnn](#). In *International Conference on Machine Learning*, pages 1863–1871.
- Ben Krause, Emmanuel Kahembwe, Iain Murray, and Steve Renals. 2019. [Dynamic evaluation of transformer language models](#). *arXiv preprint arXiv:1904.08378*.
- Kevin J Lang, Alex H Waibel, and Geoffrey E Hinton. 1990. [A time-delay neural network architecture for isolated word recognition](#). *Neural networks*, 3(1):23–43.
- Henry W Lin and Max Tegmark. 2016. [Critical behavior from deep dynamics: a hidden dimension in natural language](#). *arXiv preprint arXiv:1606.06737*.
- Tal Linzen, Emmanuel Dupoux, and Yoav Goldberg. 2016. [Assessing the ability of lstms to learn syntax-sensitive dependencies](#). *Transactions of the Association for Computational Linguistics*, 4:521–535.
- Pengfei Liu, Xipeng Qiu, Xinchu Chen, Shiyu Wu, and Xuan-Jing Huang. 2015. [Multi-timescale long short-term memory neural network for modelling sentences and documents](#). In *Proceedings of the 2015 Conference on Empirical Methods in Natural Language Processing*, pages 2326–2335.
- Mitchell P Marcus, Beatrice Santorini, Mary Ann Marcinkiewicz, and Ann Taylor. 1999. [Treebank-3](#). *Linguistic Data Consortium, Philadelphia*, 14.
- Gábor Melis, Tomáš Kočiský, and Phil Blunsom. 2019. [Mogriker lstm](#). In *International Conference on Learning Representations*.
- Gbor Melis, Chris Dyer, and Phil Blunsom. 2018. [On the state of the art of evaluation in neural language models](#). In *International Conference on Learning Representations*.
- Stephen Merity, Nitish Shirish Keskar, and Richard Socher. 2018. [Regularizing and optimizing LSTM language models](#). In *International Conference on Learning Representations*.

Stephen Merity, Caiming Xiong, James Bradbury, and Richard Socher. 2017. [Pointer sentinel mixture models](#). In *International Conference on Learning Representations*.

Tomáš Mikolov, Anoop Deoras, Stefan Kombrink, Lukáš Burget, and Jan Černocký. 2011. [Empirical evaluation and combination of advanced language modeling techniques](#). In *Twelfth Annual Conference of the International Speech Communication Association*.

Matthew Peters, Mark Neumann, Mohit Iyyer, Matt Gardner, Christopher Clark, Kenton Lee, and Luke Zettlemoyer. 2018. [Deep contextualized word representations](#). In *Proceedings of the 2018 Conference of the North American Chapter of the Association for Computational Linguistics: Human Language Technologies, Volume 1 (Long Papers)*, pages 2227–2237, New Orleans, Louisiana. Association for Computational Linguistics.

Tim Sainburg, Brad Theilman, Marvin Thielk, and Timothy Q Gentner. 2019. [Parallels in the sequential organization of birdsong and human speech](#). *Nature communications*, 10(1):1–11.

Yikang Shen, Shawn Tan, Alessandro Sordoni, and Aaron Courville. 2018. [Ordered neurons: Integrating tree structures into recurrent neural networks](#). In *International Conference on Learning Representations*.

Corentin Tallec and Yann Ollivier. 2018. [Can recurrent neural networks warp time?](#) In *International Conference on Learning Representations*.

Mariya Toneva and Leila Wehbe. 2019. [Interpreting and improving natural-language processing \(in machines\) with natural language-processing \(in the brain\)](#). In *Advances in Neural Information Processing Systems*, pages 14928–14938.

Jiacheng Xu, Danlu Chen, Xipeng Qiu, and Xuan-Jing Huang. 2016. [Cached long short-term memory neural networks for document-level sentiment classification](#). In *Proceedings of the 2016 Conference on Empirical Methods in Natural Language Processing*, pages 1660–1669.

Xunjie Zhu, Tingfeng Li, and Gerard De Melo. 2018. [Exploring semantic properties of sentence embeddings](#). In *Proceedings of the 56th Annual Meeting of the Association for Computational Linguistics (Volume 2: Short Papers)*, pages 632–637.

5 Supplementary Material

5.1 Shape parameter for Inverse Gamma distribution

We compared the performance of multi-timescale language model for different shape parameters in inverse gamma distribution. Figure 9 shows

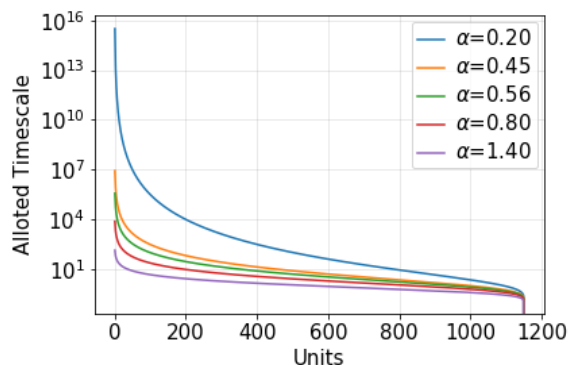


Figure 9: Assigned timescale to LSTM units of layer2 of multi-timescale language model corresponding to different shape parameter α .

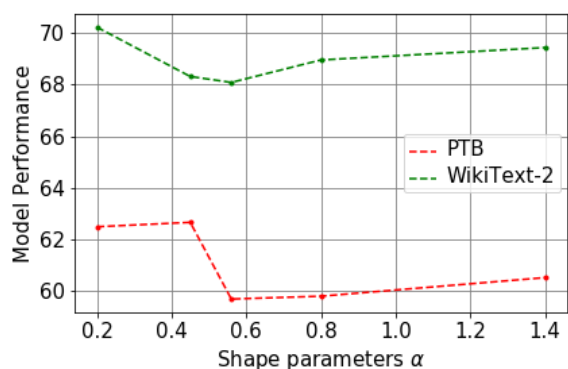


Figure 10: Performance of multi-timescale models for different shape parameters α on both PTB and WikiText-2 dataset.

timescales assigned to LSTM units of layer 2 corresponding to different shape parameters. These shape parameters cover a wide range of possible timescale distribution to the units. Figure 10 shows that multi-timescale models performs best for $\alpha = 0.56$.

5.2 Selecting the timescales for each layer

With the purpose to select proper timescales to each layer in Section 3.1, we conducted experiments on designing LSTM language models with different combinations of timescales across the three layers. We found that layer 1 (the closest layer to input) always prefers smaller timescales within the range from 1 to 5. This is consistent with what has been observed in literature: the first layer focuses more on syntactic information present in short timescales (Peters et al., 2018; Jain and Huth, 2018). We also observed that the layer 3, i.e., the layer closest to the output, does not get affected by the assigned timescale. Since we have tied encoder-

Dataset	Model	Performance
PTB	Baseline	61.64 \pm 0.28
	Multi-timescale	59.63 \pm 0.18
WikiText-2	Baseline	70.23 \pm 0.24
	Multi-timescale	68.33 \pm 0.12

Table 2: Perplexity of the baseline and multi-timescale models over 5 different training instances. Values are the mean and standard error over the training instances.

decoder settings while training, layer 3 seems to learn global word representation with a specific timescale of information control by the training task (language modeling). The middle LSTM layer (layer 2) was more flexible, which allowed us to select specific distributions of timescales. Therefore, we achieve the Multi-timescale Language Model in Section 3.1 by setting layer 1 biases to small timescales, layer 2 to satisfy the inverse gamma distribution and thus aim to achieve the power-law decay of the mutual information, and layer 3 with freedom to learn the timescales required for the current task.

5.3 Robustness of model performance

We quantified the variability in model performance due to stochastic differences in training with different random seeds. Table 2 shows the mean perplexity and standard error across 5 different training instances. The variance due to training is similar across the two models.

5.4 Experiments on WikiText-2 dataset

We performed word ablation and information routing experiments for multi-timescale model trained on WikiText-2 dataset. Figure 11 shows timescale-dependent routing in the model, same as what we observed for PTB dataset in Section 3.2.5. We also explored the rate of cell state decay across units in layer 2 of the model with different assigned timescales. We can observe that assigned timescales to the units control information routing through them, similar to PTB dataset in Section 3.2.3.

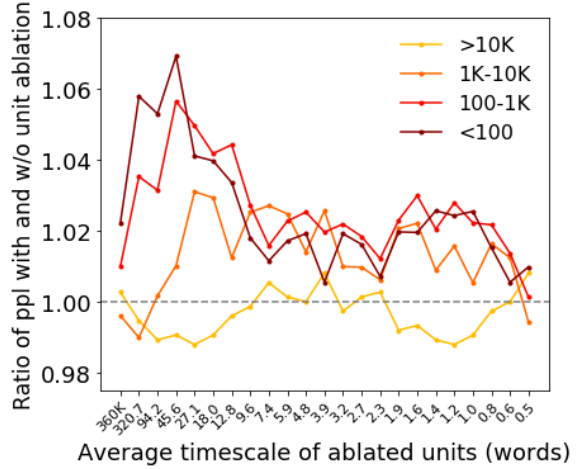


Figure 11: Information routing across different units of the multi-timescale LSTM for WikiText-2 dataset.

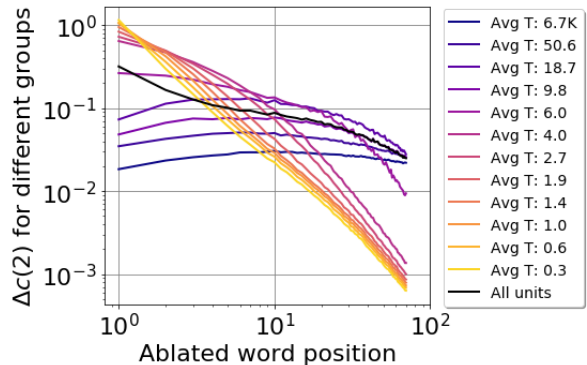


Figure 12: Change in cell states of 100-unit groups having different average timescale of layer 2 in Multi-timescale model in word ablation experiment for WikiText-2 dataset.